

ELECTRICAL MACHINE TECHNOLOGIES FOR AN ELECTRIC TAIL ROTOR DRIVE

P.H. Mellor, J. Yon, S. Williamson, J. Farman, J.D. Booker, University of Bristol, UK
M. Barber, K. Stickels, P. Brinson, AgustaWestland, UK

Abstract

This paper presents findings from an EU JTI Clean Sky funded program investigating the feasibility of driving electrically the tail rotor of a helicopter. Since the tail rotor drive is a safety critical component a major emphasis has been on the faulted behaviour of the electrical system and the realisation of a high level of integrity. Designs of two candidate fault tolerant axial-flux and radial-flux electric tail rotor motors are presented and compared. The approach adopted to model the thermal behaviour of the designs during normal and faulted operation is outlined and the impact of the aircraft mission duty on the accrued motor life described. The discussion is backed with findings from full size prototypes of the electric tail rotor motor designs.

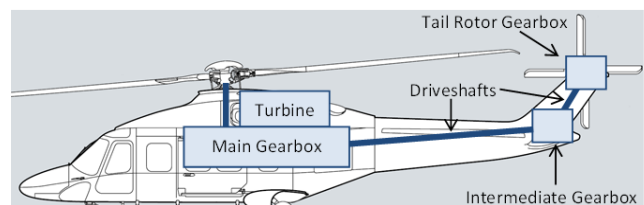
1. INTRODUCTION

This paper presents findings from the European Commission JTI Clean Sky funded project Electric Tail Drive-Modelling, Simulation and Rig Prototype Development (ELETAD). Traditionally, helicopter tail rotors are powered mechanically through a drive shaft that connects the tail rotor to the main transmission. The overall project aim is to investigate the feasibility of replacing the mechanical drive system, Fig. 1a, by an electric tail rotor (ETR) drive mounted at the back of the helicopter, with an emphasis on system faulted operation and integrity. The ETR system comprises a lightweight and compact electric motor connected via cables to a power electronic converter which acts to condition and control the power feed to the electrical machine, Fig. 1b. The input to this power converter is derived from a generator driven off the main rotor gearbox. The potential advantages of the ETR system include:

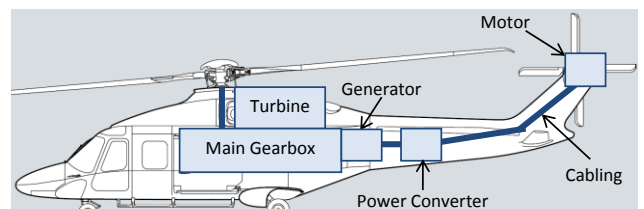
- reduced future reliance on hydraulic and oil based systems;
- low maintenance, high service life, with reduced repair and overhaul cycle impact;
- inherent torque control and power limiting directly inferred measurement of operating load
- higher system integrity, and inbuilt fault tolerance.

With the existing mechanical solution, the tail and main rotors are directly coupled through a series of high-speed shafts and gearboxes, where synchronous and closely-toleranced fixed tail rotor speed control avoids excitation of airframe and tail boom resonances. A typical peak power capability

for an aerospace gearbox is likely to be of the order of 10kW/kg. Mechanical malfunction of the tail rotor, which contains many critical parts and assemblies, and the resulting failure to provide main rotor torque reaction can lead to catastrophic loss of control of the aircraft. Consequently, the tail rotor drive is a safety critical component and its integrity is an overarching consideration. The integrity of 10^{-9} failures per flight hour dictates a regular inspection, maintenance and replacement regime for the existing mechanical system, the frequency of which is based on a knowledge of the aircraft usage. For the electrical drive alternative to be viable it will need to be proven to deliver the integrity and performance requirements whilst offering improved service life.



a) Traditional mechanical tail rotor power transmission



b) Electrical tail rotor (ETR) power transmission

Figure 1. Tail rotor power transmission alternatives

The objectives of the Clean Sky project presented in this paper includes prototyping a full scale high power density and high integrity ETR motors to a specification representative of a medium sized twin-

engined helicopter. Table I lists the original target requirements. The test benchmark for the ETR motor is that it should be capable of sustaining a 1 kNm torque output for a period of two hours. The sustained specific torque capability exceeds 20Nm/kg, based on the weight of the active stator and rotor elements, and is challenging for an air-cooled machine. In addition to a low overall weight the volumetric envelope of the design is also tightly constrained. The machine is to be power electronic controlled, however, the design voltages should be compatible with the standard 115 Vrms, 400 Hz aircraft a.c. supply system.

Table I. Target Motor Requirements

Specific output (continuous output per weight of active elements)	>3.5 kW/kg
Nominal rotational speed	1700 rpm
Nominal torque (sustained continuous duty)	1 kNm
Peak transient torque	>2 kNm
Electrical system	115 V, 400 Hz

2. SYSTEM ARCHITECTURE CONSIDERATIONS

There are major differences in the operation and faulted behaviour of the mechanically driven and electrically driven tail rotor systems depicted in Fig. 1. The mechanical transmission effectively acts as a constant speed power source where the instantaneous power draw and thrust is defined by the aerodynamic operating conditions of the tail rotor fan. The thrust is solely controlled by varying the pitch of the rotor blades and a sudden large increase in the pitch demand may, in the extreme, cause the rotor to stall resulting in a large power surge to be transmitted along the mechanical linkage. In contrast the electrical drive operates as a controlled torque source, the magnitude of which is set by the demanded level of motor current. Fixed speed operation is realised by incorporating an outer control loop which dynamically adjusts the demanded motor torque to maintain the desired speed. Thus it is not possible to inadvertently overload the electrical drive; a sudden increase in the aerodynamic load would cause the rotor speed to fall rather than drive it into stall. As a result the loading of the electrical tail drive is precisely controllable and can be limited to preserve the integrity of operation. Furthermore, the ETR system lends itself to the multiplex fault tolerant configuration explored in this paper, comprising independently controlled power channels which evenly share the load in normal operation.

The accelerated life testing and qualification process of the substitute electrical drive system is less well

established. Failures in electrical components are dominated by thermal cycling rather than cyclic load accumulation. In the power electronic converter, a dominant source of failure results from the packaging of the power semi-conductor switches where thermal cyclic stresses causes cracking in the device to substrate mounting and lifting of the bond wire connections [1]. The d.c. link filter capacitor is also a weak link due to its commonality across multiple phases driven from a single d.c. link [2]. Ageing in electrical machines is primarily a result of thermoelectric and mechanical degradation of the winding insulation and connections. Insulation deterioration follows an Arrhenius relationship with every 10 °C increase in temperature halving the lifetime and is exaggerated with dielectric stress, mechanical vibration and humidity [3]. Based on indicative reliability figures found in the literature, the Mean Time Between Failure (MTBF) for the simplex electrical power transmission indicated in Fig. 1b was estimated at 1.6×10^{-4} hr [4]. A quadruplex system comprising four separate electrical power channels has therefore been developed to meet the safety critical availability target.

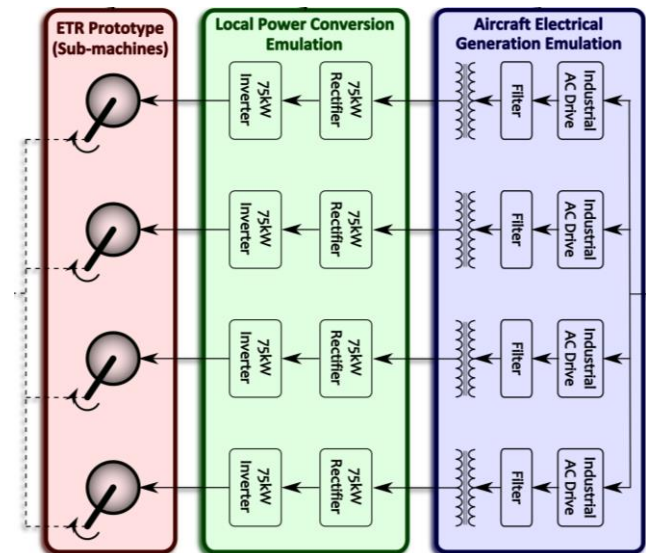


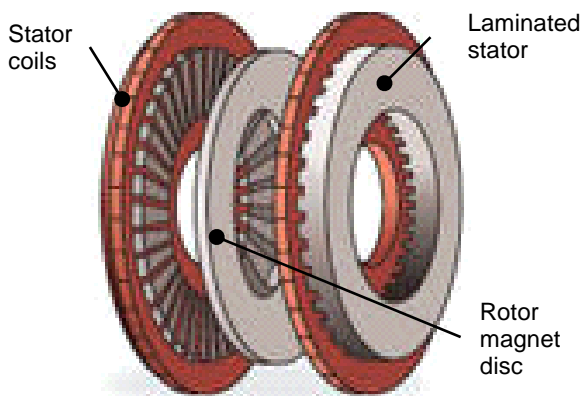
Figure 2. Four channel electrical system architecture

Fig. 2 presents an overview of the electrical system architecture that is being employed in the test characterisation of the ETR electrical machine. The arrangement consists of four independent electrical power supply and control channels, each rated at 75kW a minimum 50% transient overload capability. A power channel would be isolated should a failure in the generator supply, power electronics or a motor winding occur. The method of isolation would be to either electrically disconnect the supply to the motor sub-machine, or in the case of a winding or power semiconductor device short circuit fault, apply a balanced short-circuit to the terminals of the motor sub-machine [5,6]. The design of the fault-tolerant permanent magnet electrical machine is such that it

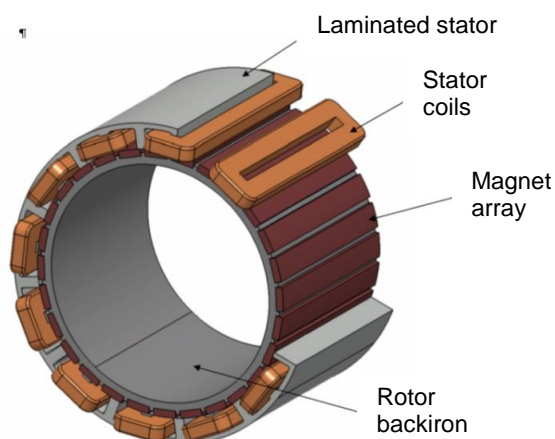
would be able to sustain a short circuit current without an excessive temperature rise in the effected coil and there should be sufficient thermal isolation between the motor sub-modules to prevent the fault propagating to other winding coils [7].

3. SELECTED ELECTRICAL MACHINE TYPES

Permanent magnetic (PM) brushless electric machines tend to have superior torque/power density and efficiency characteristics, and are particularly suited to highly dynamical load duty cycles. They are the preferred technology for electric aircraft actuation, industrial servo drives and electric vehicle wheel drives [8,9]. Candidate electric tail rotor motor designs were down-selected to two candidate brushless a.c. PM machine formats: the double airgap axial-flux and modular wound radial-flux, and these offered the highest potential torque-density. Whilst other higher specific output technologies, such as transverse flux motors, exist these have yet to reach a sufficient maturity in terms of manufacture for consideration here. Fig. 3, presents the two alternative motor topologies.



a) Double air gap axial-flux topology



b) Modular wound radial-flux topology

Figure 3. Down selected axial-flux and radial-flux electrical machine topologies

The axial flux design comprises two wound stator assemblies stator located at either side of a central permanent magnet disc. The radial flux topology consists of an inner permanent magnet array surrounded by a single stator lamination into which twelve coils are inserted. Despite the fundamental differences in these topologies, there are similarities between the two approaches:

- The axial-flux and radial-flux design processes seek to maximise the available active area for force production and the radius at which this occurs within the constraints of a given housing volume and, as a result, these topologies have the highest specific torque. The cooling and mechanical arrangements are, however, more complex. Continuous specific outputs for air-cooled versions of these types of motor exceed 10Nm/kg making them highly attractive for the tail rotor application. [10,11].
- Open slot stator designs are possible which greatly simplify the winding process, leading to excellent copper utilisation, high electrical loading (ampere stream) for a given power loss and mechanical robustness. Importantly, this need not incur high levels of undesirable torque ripple [12]. The lack of a tooth tip, however, means that the method employed to secure the winding within the slot can potentially introduce a thermal barrier, and a.c. loss effects in the winding and rotor are greater.

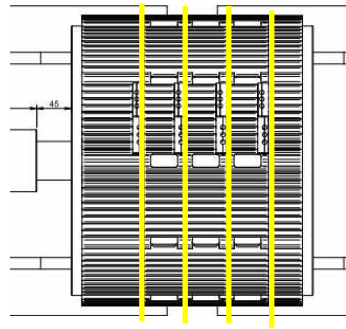
Fault tolerance is incorporated in a different manner for the axial- and radial-flux variants. In the case of the axial flux topology, multiple machines can be stacked axially sharing a common shaft. To achieve a quadruplex system four rotor discs and eight stators were fabricated in a common housing. The radial flux machine utilises a modular winding concept where each coil making up the stator has a dedicated slot and magnetic circuit. Whilst the design ensures there is minimum electrical and magnetic interaction between the phase coils there is a degree of thermal coupling across the four independent motor channels. Four independent electrical machines can be created by arranging the twelve coils into four sets of 3-phase windings.

Independent design studies on the axial-flux and radial-flux machine indicated they would have comparable performances and similar overall weights. Further, the axial flux was a more mature design being based on previous machines of similar construction whereas the radial-flux was a new concept and therefore carried greater development risk. As a result it was decided to manufacture prototypes of both machines. Figs 4 and 5 show the

two prototypes fault-tolerant axial-flux and radial-flux ETR motor designs and are currently under test. The physical separation of the four machine modules are clearly identified in axial-flux motor assembly, Fig 4b. The radial flux machine is more integrated with separately fed phase coils sharing a common rotor and a common stator lamination, Fig. 5b. The mounting and shaft arrangements of the prototypes were selected to suit the dynamometer test setup and are not representative of the final aircraft installation. Compared to the axial flux machine, the radial-flux prototype had a smaller outer diameter (365 mm versus 375 mm) but a longer total length (314 mm versus 290 mm). The total weights of the electromagnetically active materials which made up the final designs were almost identical, however the relative contributions to the total active weight differed, Table II. The four stacked stator core and winding assemblies that make up the axial flux machine are heavier than the radial flux core back and windings. However the double-sided disc structure of the axial-flux eliminates the need for a back iron to return the rotor flux and is correspondingly lighter. The final active weights of the designs were 18% greater than the original targets. Readily available grades of permanent magnet and silicon iron laminations were used for the prototypes and there would be scope for weight reduction in using higher performance materials.



a) Axial-flux prototype including dynamometer mounting arrangement



b) Plan view indicating the axial division of motor sub-modules

Figure 4. Axial-flux prototype machine



a) Radial-flux prototype including dynamometer mounting arrangement



b) End view indicating the independent coil connections

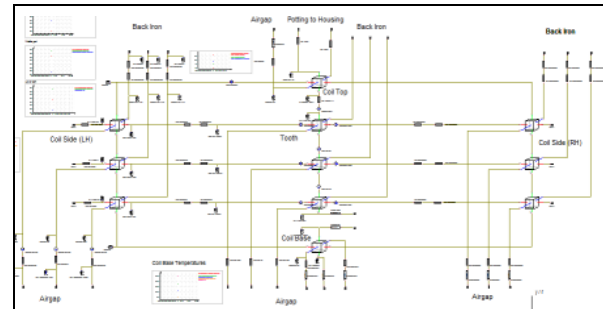
Figure 5. Radial-flux prototype machine

TABLE II PERCENTAGE WEIGHT BREAKDOWN OF ACTIVE MATERIAL USED IN THE TWO PROTOTYPE DESIGNS

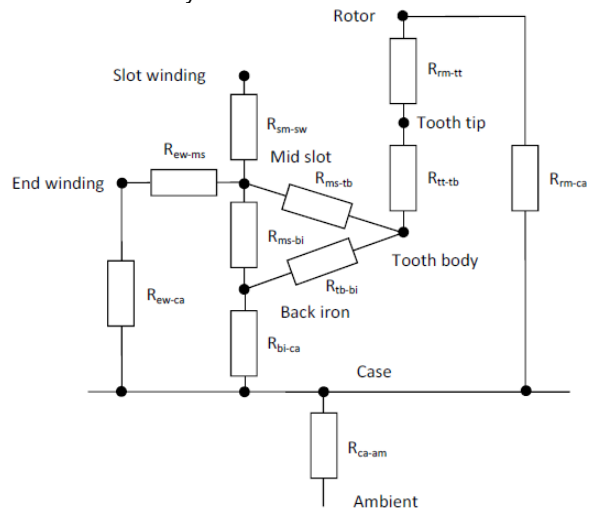
Active component	Axial-flux	Radial-flux
Stator core	40 %	34 %
Winding copper	36 %	32 %
Permanent magnet	24 %	25 %
Rotor back iron	N/A	9 %

4. THERMAL MODEL DEVELOPMENT

The ETR design brief is highly challenging will not be met using traditionally conservative approaches to thermal design and rating. Underpinning the design analyses is a suite of bespoke thermal modelling tools catering for the axial-flux and radial-flux topologies. Lumped element thermal representations of the two machine topologies were constructed. The approach separates the geometry of the machine into a small a number of bulk regions, each represented as a single lumped temperature node with an associated thermal capacitance and loss. The heat transfer between neighbouring nodes is modelled as a bulk value of thermal resistance found from analytical and numerical thermal analyses [13].



a) 10 node representation of axial-flux motor winding and stator core assembly



b) 8 node reduced order model for radial-flux modular motor sub-assembly

Figure 6. Lumped element thermal model applying to the two topologies



Figure 7. Example motorettes used to calibrated the thermal analyses

The proposed reduced order thermal model structure is shown in fig. 6 for the two machines and has been developed based on knowledge of the heat transfer paths in the respective machines. In the case of the radial flux-machine it was found the temperatures of the stator winding and surrounding core could be adequately modelled in terms of a reduced order network comprising only six bulk regions. A seventh node is used to model the temperature of the case, whilst an eighth node is used to represent the temperature of the permanent magnets on the rotor.

The developed thermal models were refined and validated through tests on sub-machine assemblies prior to the manufacture of the full-scale prototypes. In the case of the axial-flux machine, a single motor module was prototyped and tested, and for the radial flux design, a number of single coil motorettes were constructed, fig. 7. Each motorette represented a 30 degree sector of the stator assembly and were constructed with the same materials, manufacturing processes and insulation systems as intended in the final prototype.

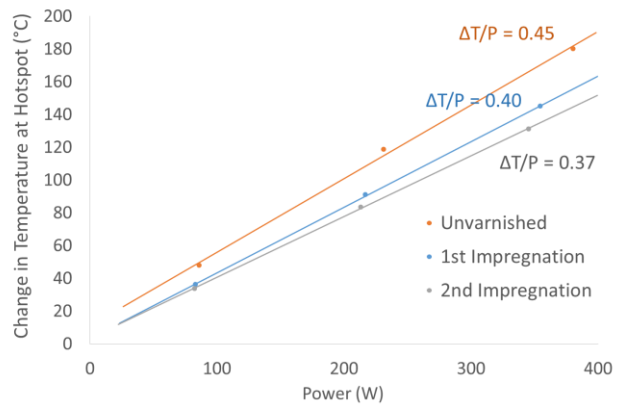


Figure 8. Typical results obtained from motorette thermal tests

Fig. 8 presents typical data obtained taken from the motorette thermal testing. The figure plots the peak measured coil temperature as a function of loss from which the dissipative capabilities of the winding coil can be calibrated. Such motorette tests proved valuable in determining the bulk thermal properties of the winding regions [14] and the interface thermal resistance between the coil and the surrounding slot across the protective slot liner layer. Further, the results indicate how the stages of varnish impregnation of the motor windings would improve the thermal performance.

The radial-flux fault tolerant machine can be viewed as a set of electromagnetically and thermally independent machine units orientated around the stator circumference. The thermal network for the full fault tolerant machine will therefore share common case and rotor nodes, with separate sets of the remaining nodes to model each sub-unit. In effect, the model is divided into two sub networks; one representing the faulted unit(s) and the other representing the remaining healthy winding coils assuming balanced loading between the healthy units. This is illustrated in Fig. 9.

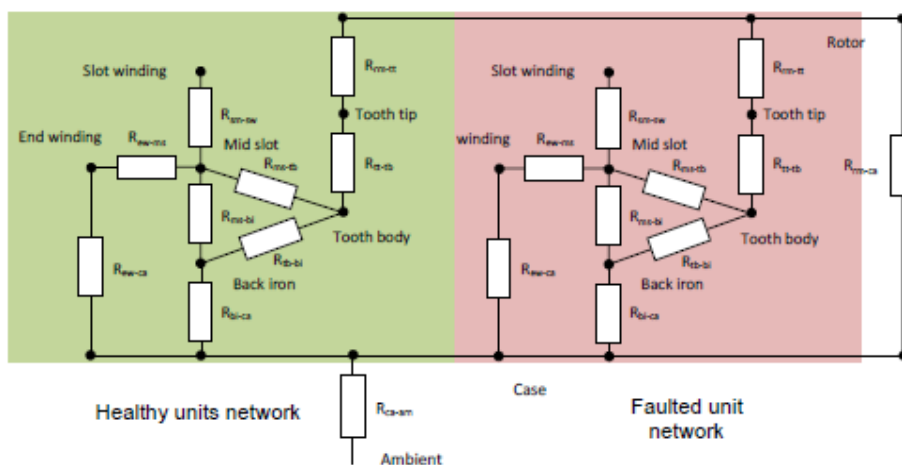
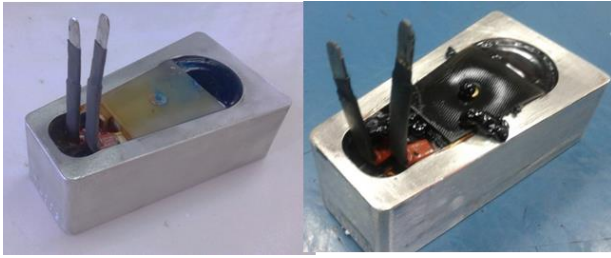
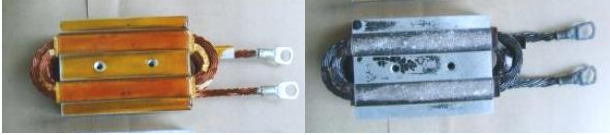


Figure 9. Reduced order thermal model for the radial flux machine with a faulted motor sub-unit

5. WINDING INSULATION LIFE ASSESSMENT



a) Axial-flux insulation test samples



b) Radial-flux insulation test samples

Figure 10. Motorette samples, before and after insulation life testing

A number of formulations exist for estimating the accrued life of the winding insulation system when subjected to thermal stresses. In general, it is considered that insulation system degradation occurs due to chemical reactions whose characteristic rate varies with temperature according to the Arrhenius law. Insulation systems are usually classified as having a minimum life at a particular temperature, for example 20,000 hours at 180°C (Class H). This life is typically determined from accelerated life tests where an end of life criterion is measured at a fixed elevated temperature. This measured lifetime L_n , is given by [15]:

$$(1) \quad L_n = A \exp\left(\frac{B}{T_n}\right)$$

with the material aging constants A , B obtained experimentally and T_n is the test absolute temperature in Kelvin. From (1) a plot of the logarithmic of measured lifetime against the reciprocal of absolute temperature will be linear and can be used to determine the life model parameters A, B . The constant A is not explicitly required as it is implicit that a particular life will be achievable at the class temperature rating of the insulation system. The accrued life over a particular duty can therefore be found using:

$$(2) \quad \Gamma = \int \exp\left(\frac{B}{T_C} - \frac{B}{T(t)}\right) dt$$

where T_C is the specified class temperature and $T(t)$ is the instantaneous insulation temperature, both in Kelvin. The insulation system will be judged to have reached its end of life when the totalled accrued life found using (2) exceeds the specified life at the insulation class temperature.

Sub-assembly testing was also used to determine the parameters of an insulation life model used in the

reliability analyses. Statistically relevant numbers of motorette winding samples were manufactured using the same grade of wire and insulation system to be used in the final prototypes. Samples representative of both motor geometries were constructed, Fig. 10.

Each sample batch were subjected to multiple test cycles of a prolonged exposure to elevated temperatures, 1 hour vibration at 1.5 G and a 48 hrs exposure to 30 °C and 85% humidity according to standards: IEC 60034-18-31 (1999), and IEC 60216-1 (2001). At the end of each test cycle the insulation system integrity was monitored through measurements of high voltage insulation resistance, capacitance and dielectric loss. Fig. 11 indicates the outcome of the life assessment on a batch of motorette samples when subjected to a 220 °C, 28 day duration test cycle. A noticeable change in winding insulation characteristics occurred after eight 28 day test cycles although full insulation breakdown did not occur until after ten 28 day cycles. The results indicate the chosen insulation system should operate for 5,400 hrs at this temperature before any noticeable degradation of life would be observed. From the motorette accelerated ageing tests of the coefficient B used in (2) was obtained to be 14,200K.

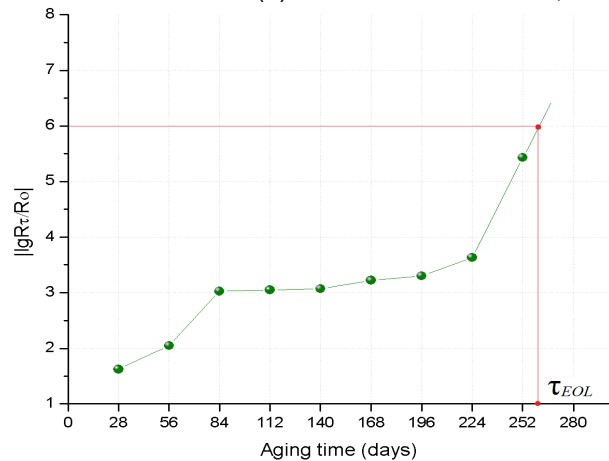
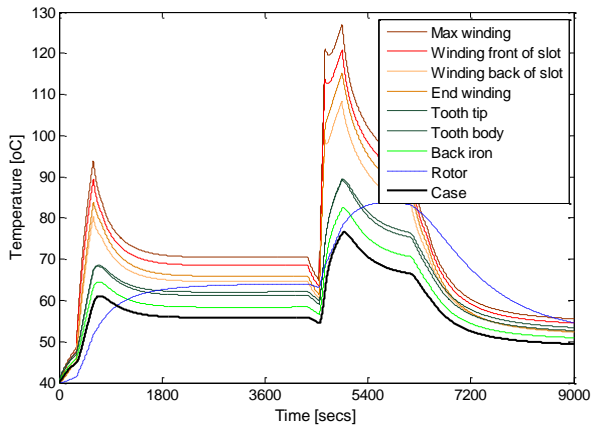


Figure 11. Example of insulation life test results

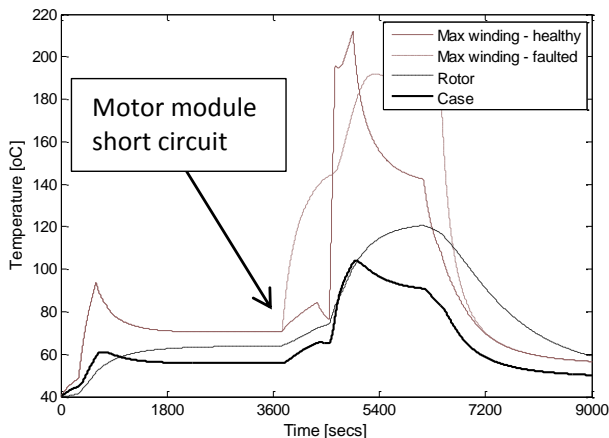
6. THERMAL MODEL RESULTS

The developed thermal and insulation life models have been applied to evaluate the performance of the ETR motor designs against the benchmark sustained performance criteria and over representative flight missions. Normal and faulted operation were considered. Fig. 12a presents a simulation of the radial-flux motor temperatures over a typical search and rescue flight mission during normal operation. The mission comprises a vertical take-off, high speed cruise to the point of deployment, a loitering and hovering phase whilst executing a rescue pick-up and a return to base. The scenario of a fault occurring an hour into the mission and prior to the important rescue phase was

also considered, Fig. 12b. On detection of a fault, for example due to a shorted power semiconductor in the power converter, in mitigation the system imposes a short circuit on the phases of the motor sub-machine power channel. As a result the load on each of the remaining 3 motor sub-machines will be increased by over 33% and the machine will need to dissipate the higher losses associated with short circuited operation of the faulted module. Due to the fault tolerant design of the machine the mission will not be compromised, although the final winding temperatures will be elevated. With a more demanding mission or in the case of a fault in a second power channel the mission may need to be terminated prematurely, however the progressive redundancy of the electrical system would mean the aircraft could be safely landed. The thermal modelling work has also indicated the bench mark sustained continuous output of 1 kNm for two hours is releasable from the radial-flux machine design however the accrued winding insulation life would be in the order of 100 hours.



a) Reduced order thermal network prediction, normal operation



b) Faulted operation with one motor module short circuited (only maximum winding temperature shown)

Figure 12. Evaluation of motor temperatures over a typical flight mission

7. PROTOTYPE MACHINE TESTS

Characterisation tests on the axial-flux and radial-flux machines are ongoing at the time of writing of this paper. The initial characterisation procedure involves measurement of the electrical parameters, measurement of the ETR motor losses and temperatures during open circuit operation and with one or more of motor sub-modules short-circuited. The prototypes will then be powered from four separate 75 kW inverter supplies, one for each motor sub-machine using the arrangement indicated in fig. 2. These full system tests will be used to establish the sustained output capabilities at increasing levels of load. Finally the motor performance will be evaluated over representative mission cycles.

The radial-flux prototype was inadvertently supplied with a faulted winding coil. This provided an opportunity to confirm the thermal isolation between the motor phases of the fault tolerant design. Fig. 13 plots the measured winding temperatures during no-load operation. In the prototype the thermocouples are fitted to either end turn of the twelve coils. The two thermocouples relating to the faulted coil can be seen to give an elevated temperature compared to the eleven other coils. The fault did not propagate to the remaining eleven coils which had a similar spread of temperatures. On subsequent investigation the fault was found to be a result of an inter-turn short circuit between one or more of the multiple parallel stranded conductors that make up the winding. The nature of the connection led to initially a high level of loss, as indicated by the rapid rise in the faulted coil temperature, however the fault was observed to be self-limiting at the test progressed.

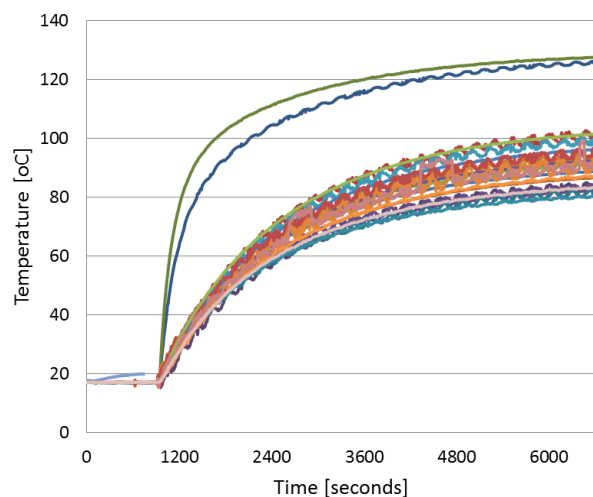


Figure 13. Measured winding temperatures with a faulted coil installed (two thermocouples fitted to each coil)

8. DISCUSSION

The design of a full-scale helicopter electric tail rotor (ETR) motor that is engineered for flight-critical operation and packaged in a manner that is representative of an aircraft installation poses a significant challenge. Any replacement system must be weight competitive with and at least as reliable as the existing mechanical solution, whilst offering demonstrable performance and whole-life cost benefits. These challenges may be addressed by considering a direct drive solution capitalising on recent developments in high performance electrical machine design. Two high specific output topologies of brushless AC permanent magnet electrical machines have been identified as being suitable candidates for the ETR requirements; the double airgap axial flux and the modular wound radial flux configurations. Candidate designs of both these machine topologies were developed in detail and unexpectedly yielded solutions with very similar active weights. As no distinguishing difference in weight or size emerged prototypes of both machine types have been constructed and are currently under test evaluation.

The load power spectrum experienced by a tail rotor drive has a wide ranging peak-to-mean duty profile which suggests that a compact electrical machine with a constrained equivalent continuous rating would be a potential solution. In order to fully understand the implications of down-sizing the continuous capability the design toolset should incorporate a thermal model capable of predicting critical temperatures such as those of the winding for typical dynamic load missions. The use of a lumped parameter thermal network has been shown to be effective in this regard. The reduced order form of a lumped thermal network can be readily adapted to include temperature prediction during faulted operation. Additionally, a means for assessing the accrued life under normal and abnormal loading regimes ideally should be incorporated in the design synthesis.

The safety-critical demands of the application can be addressed by designing a redundant fault tolerant electrical system, where the ETR motor comprises a number of thermally and magnetically independent sub-units. The approach ensures an electrical failure in one unit would not inhibit the operation of the others. The findings have indicated that a four channel system would provide the required level of integrity and in many cases the loss of one of these channels would not compromise the successful completion of the flight mission. In the case of a fault in a second power channel the mission may need to be terminated prematurely, however the progressive redundancy of the electrical system would mean the aircraft could be safely landed.

The electric tail rotor concept, if proven to be technically and economically viable, would eliminate the need for the complex and costly high-speed shaft and gearbox assemblies and would significantly reduce maintenance requirements. In comparison with a direct mechanical connection, the electrical solution offers increased freedom to decouple tail rotor control from the main rotor such that excitation of airframe resonances may be avoided and acoustic noise significantly reduced. Electrical power conversion technologies are reaching a high degree of maturity in fixed wing aircraft with the installed electrical power exceeding 1MW on new aircraft platforms. More electric technologies like this are likely to enable exciting new innovations in vertical take-off aircraft in the future.

REFERENCES

- [1] Aten, M.; Towers, G.; Whitley, C.; Wheeler, P.; Clare, J.; Bradley, K.; "Reliability comparison of matrix and other converter topologies," IEEE Trans. Aerospace and Electronic Systems, 2006, Vol. 42: pp. 867-875.
- [2] Chan, F.; Calleja, H.; "Design strategy to optimize the reliability of power converters," 11th IEEE Int. Congress in Power Electronics, CIEP 2008, 2008: pp. 128-132.
- [3] Bell, S.; Sung, J.; "Will your motor insulation survive a new adjustable frequency drive?," IEEE IAS 43rd Conf. in Petroleum and Chemical Industry, 1996: pp. 125-130.
- [4] Farman, J.; "Electric Tail Rotor Drive for the More-Electric Helicopter: A Feasibility Study", PhD, University of Bristol, 2013.
- [5] Mellor, P.H.; Burrow, S.G.; "Control of a brushless PM traction drive following a winding or power semiconductor failure", SAE Transactions Journal of Engines, July 2005.
- [6] Nall, S.; Mellor, P. H.; "A compact direct-drive permanent magnet motor for a UAV rotorcraft" 4th IET Conf. on Power Electronics, Machines and Drives, , 2008: pp. 245-249.
- [7] Mecrow, B.C.; Jack, A.G.; Haylock, J.; Coles, J.; "Fault-tolerant permanent magnet machine drives", IEE Proc. Electric Power Applications, 1996, Vol. 143, (6): pp.437-442.
- [8] Gerada, C.; Bradley, K.J.; "Integrated PM Machine Design for an Aircraft EMA", IEEE Trans. Industrial Electronics, 2008, Vol. 55, (9): pp. 3300 -3306.
- [9] Rahman, Z.; "Evaluating radial, axial and transverse flux topologies for 'in-wheel' motors" Power Electronics in Transportation, 2004: pp. 75-81.
- [10] Rahman, K.M.; Patel, N.R.; Ward, T.G.; Nagashima, J.M.; Caricchi, F.; Crescimbin, F.; "Application of Direct-Drive Wheel Motor for Fuel Cell Electric and Hybrid Electric Vehicle Propulsion System", IEEE Trans. Industry Applications, 2006, Vol. 42, (5): pp. 1185-1192.
- [11] Giulii Capponi, F.; De Donato, G.; Caricchi, F.; "Recent Advances in Axial-Flux Permanent-Magnet Machine Technology", IEEE Trans. Industry Applications, 2012, Vol. 48, (6): pp. 2190-2205.
- [12] Wrobel, R.; Mellor, P.H.; "Design Considerations of a Direct Drive Brushless Machine With Concentrated Windings", IEEE Trans. Energy Conversion, 2008, Vol. 23, (1): pp. 1-8.
- [13] Boglietti, A.; Cavagnino, A.; Staton, D.; Shanel, M.; Mueller, M.; Mejuto, C.; "Evolution and Modern Approaches for Thermal Analysis of Electrical Machines", IEEE Trans. of Industrial Electronics, 2009, Vol. 56, (3), pp. 871-882.
- [14] Simpson, N., Wrobel, R., Mellor, P.H., "Estimation of Equivalent Thermal Parameters of Impregnated Electrical Windings", IEEE Trans. Industry Applications, 2013, Vol. 49, (6), pp. 2505-2515.
- [15] Dakin, T. W.; "Electrical Insulation Deterioration Treated as a Chemical Rate Phenomenon", AIEE Trans., Part 1, 1948.